ELSEVIER

Journal of Chromatography A, 845 (1999) 293–302

JOURNAL OF CHROMATOGRAPHY A

Study of hydroxyapatite aggregation in the presence of potassium phosphate by centrifugal sedimentation field-flow fractionation

Argyro Athanasopoulou, Dimitrios Gavril, Athanasia Koliadima, George Karaiskakis*

Department of Chemistry, University of Patras, 26500 Patras, Greece

Abstract

The aggregation of hydroxyapatite (HAP) in the presence of potassium phosphate was studied by the centrifugal sedimentation field-flow fractionation technique. The variation of the number average diameter of HAP particles with the potassium phosphate (K_3PO_4) concentration, as well as with the time led to the determination of rate constants for the bimolecular process of aggregation. At concentrations of K_3PO_4 higher than $5 \cdot 10^{-2} M$, the aggregation of HAP particles led to a bimodal distribution with two populations of particles, thus making possible the division of the polydisperse HAP particles into two narrower fractions by the centrifugal sedimentation field-flow fractionation technique.

Keywords: Field-flow fractionation; Hydroxyapatite; Potassium phosphate

1. Introduction

Field-flow fractionation (FFF) is a highly promising tool for the characterization of colloidal materials [1–13]. The special subtechnique of centrifugal sedimentation FFF (SdFFF) is particularly effective in dealing with colloidal particles in the diameter range from 0.02 to 1 μm, using the normal or Brownian mode of operation (up to 100 μm using the steric-hyperlayer mode). The normal mode of operation is based on the balance reached between crossflow induced convection, driving the samples towards the accumulation wall, and molecular diffusion in the opposite direction. Eventually a steady state is reached where the sample is differentially distributed by the accumulation wall. Since the equilibrium distribution will determine the average velocity for a sample zone eluted through the channel, the sample components elute in order of diffusion coefficient, i.e. the smallest components elute first.

When the average distance from the accumulation wall, predicted by the balance of convection and diffusion, is exceeded by the particle radius an additional mechanism has to be considered, the steric-hyperlayer effect [1], which causes a shift in the elution order so that the largest particles elute first.

Not only is resolution high with the normal sedimentation FFF but separation occurs on the basis of differences in effective mass according to well-defined theoretical principles, and particle size and density parameters can be estimated directly from the FFF experiments in terms of the measured elution volumes. Since SdFFF is a true sedimentation equilibrium process, it can provide rigorous measurements of solute molecular mass or particulate mass of submicron colloidal species. In contrast, most

*Corresponding author. Tel.: +30-61-997109/997144; fax: +30-61-997118/997110.

E-mail address: gkaraisk@upatras.gr (G. Karaiskakis)

0021-9673/99/$ – see front matter
PII: S0021-9673(99)00244-7

conventional centrifugal methods are based on sedimentation velocity, which is affected by the viscosity of the liquid medium and the shape of the solutes or particulates. Density gradient equilibrium sedimentation techniques provide information only on density, whereas the sedimentation equilibrium approach in SdFFF gives particle size information as well.

Higher resolutions and shorter analysis times can be provided by SdFFF than by conventional centrifugal techniques because of the different separation mechanisms and sedimentation distances associated with these two separation methods. While centrifugal methods have a limited peak capacity, peak capacity in SdFFF is much larger.

One of the most important colloidal processes, and one that is generally quite difficult to characterize, is the aggregation of single particles to form complex aggregates. Aggregation generally is a common phenomenon for both natural and industrial colloids. However, the resolving power of SdFFF has not been fully focused on the separation and characterization of colloidal aggregates. The clearest demonstration of the ability of SdFFF to separate aggregated colloids was reported in 1980 [14], in which a complex biomaterial sample was shown to emerge a singlet, doublet, and higher-order aggregated viral rods. However, in some more recent studies undertaken to characterize polystyrene and polymethylmethacrylate latex samples using SdFFF [3], a series of peaks was observed, suggestive of low order aggregation. In pursuing these studies it was found that SdFFF provides extraordinary details on both the aggregates and the aggregation process. Recently it was found [12] that the SdFFF technique can be applied successfully for the aggregation study of polydisperse, irregular hydroxyapatite (HAP) particles. The selection of hydroxyapatite as a model sample is due to the fact that HAP [$Ca_5(PO_4)_3OH$] is the form of calcium phosphate which is precipitated in a wide range of physiological and pathological processes; proteins are invariably implicated in the deposition of HAP from biological fluids [15]. For example, HAP is deposited in close association with proteins in bone [16], in renal calculi [17], on artificial heart valves [18] and in encrusting deposits on urinary catheters [19]. By analogy with other particle-reinforced composites, the desirable or undesirable physical properties of these deposits will depend, at least in part, on the sizes and shapes of the HAP crystals.

In the present work the reversible aggregation of HAP in the presence of potassium phosphate, which leads to division of the polydisperse HAP particles into two narrower fractions, is further investigated by the SdFFF technique.

2. Experimental

2.1. Materials

The model sample of hydroxyapatite, which was kindly donated by Dr. J. Kapolos, had polydisperse, irregular plate-like particles, whose morphology was studied by means of a Phillips CM-20 transmission electron microscope at 200 kV. The Fourier transform IR pattern of the sample corresponded to that of a well crystallized HAP; peaks attributable to other solid phases were not present in the spectrum.

The carrier was triply distilled water containing 0.5% v/v of a low-foaming, low-alkalinity, phosphate-, chromate-, and silicate-free detergent FL-70 (from Fisher) and 0.02% w/w sodium azide as bacteriocide. The electrolyte used was potassium phosphate monohydrate purum from Fluka.

2.2. Apparatus and procedure

The dimensions of the SdFFF system, which has been described in detail elsewhere [12], were 38.4× 2.35×0.0197 cm with a channel void volume of 1.68 ml, measured by the elution of the non-retained peak of sodium benzoate. The outside wall of the channel was bare, polished Hastelloy C alloy, which is principally Ni (56%) with 15% Cr, 17% Mo, 5% Fe, 4% W, and traces of Mn and Si. The radius of rotation was 6.85 cm. The analysis was performed with a Gilson Minipuls 2 peristaltic pump coupled with a Gilson model 111 UV detector operated at 254 nm and a Linseis model L6522 recorder.

Aggregation and disaggregation of HAP particles in the presence of potassium phosphate were investigated experimentally by measuring their number average diameters using the SdFFF technique as a function of time and electrolyte concentration as follows: 100 μl of 3 mg ml^{-1} HAP suspension,

which was kept thermostated at 25°C while it was continuously agitated, were injected quickly at various time intervals into the SdFFF column, and then analysed by the known procedure described elsewhere [12]. For the aggregation study of HAP particles at various concentrations of potassium phosphate using SdFFF, 100 μl of 3 mg ml^{-1} sample were injected directly into the channel using as carrier the detergent FL-70 with various concentrations ($5\cdot10^{-3}$ *M*, $1\cdot10^{-2}$ *M* and $5\cdot10^{-2}$ *M*) of K_3PO_4. In all experiments of the present work the flow-rate (140 ml h^{-1}), the relaxation time (10 min), and the field strength (360 rpm) were kept constant during the analysis time. The obtained fractograms for the aggregation of HAP at various electrolyte concentrations, as well as at various times for the potassium phosphate concentrations which are lower from the critical electrolyte concentration ($5\cdot10^{-3}$ *M* and $1\cdot10^{-2}$ *M*) consisted of one peak (see Fig. 1), while those for the aggregation of HAP in the presence of $5\cdot10^{-2}$ *M* K_3PO_4 at various times consisted of two peaks (see Fig. 2), which correspond to two fractions of the polydisperse HAP sample.

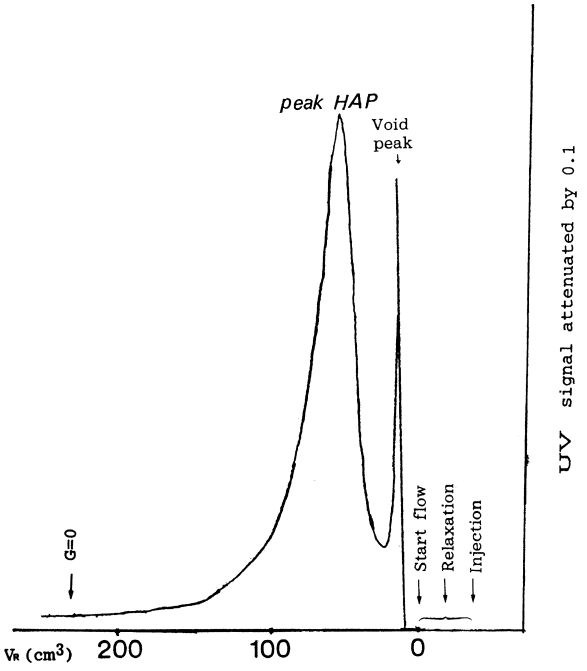

Fig. 1. Fractogram of HAP particles obtained by SdFFF in the presence of $5\cdot10^{-3}M$ K_3PO_4. Sample 100 μl; flow-rate = 140 ml h^{-1}; relaxation time = 10 min; rpm = 360.

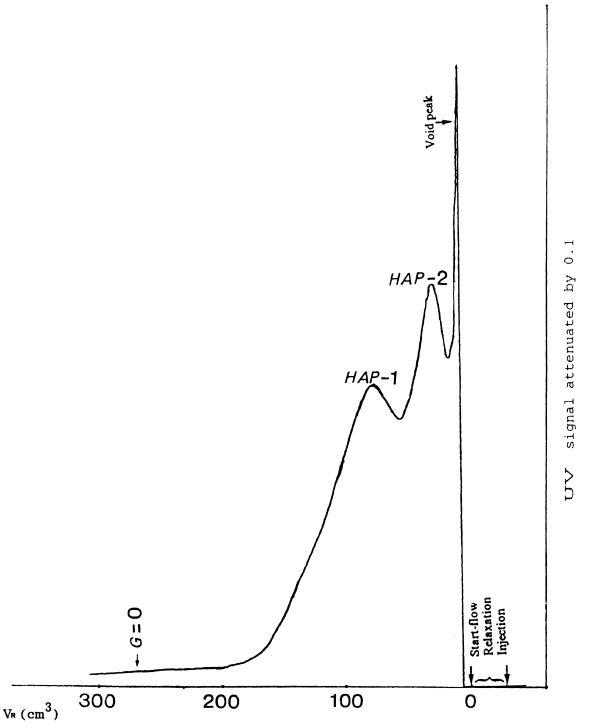

Fig. 2. Fractogram of HAP particles consisted of two peaks (HAP-1 and HAP-2), which was obtained by SdFFF in the presence of $5\cdot10^{-2}M$ K_3PO_4 (t = 258.5 h). Sample 100 μl; flow-rate = 140 ml h^{-1}; relaxation time = 10 min; rpm = 360.

3. Results and discussion

In the normal mode of SdFFF the measured retention volume V_{Ri} is directly related to the diameter d_i of a spherical colloidal particle or to the equivalent spherical diameter d_i, i.e. to the diameter of a sphere of equal volume for nonspherical particles and to the longest axis for the plate-like particles of HAP [12]:

$$d_i = \left(\frac{36kT}{\pi G w V_o \Delta\rho}\right)^{1/3} \cdot V_{Ri}^{1/3} = \lambda V_{Ri}^{1/3} \quad (1)$$

where k is the Boltzmann constant, T is temperature, G is the angular acceleration, w is the channel thickness, V_o the void volume of the SdFFF channel,

$\Delta\rho$ is the absolute value of particle density minus carrier density, and $\lambda = (36kT/\pi GwV_o\Delta\rho)^{1/3}$.

For polydisperse samples, as is the case here, the number average particle diameter d_N is determined using an appropriate computer program by the expression [10]:

$$d_N = \frac{\sum_i d_i N_i}{\sum_i N_i} = \frac{\lambda\left[\sum_i N_i V_{Ri}^{1/3}\right]}{\sum_i N_i} \quad (2)$$

where N_i is the number of particles with constant diameter d_i.

The variation of d_N for the HAP particles with the potassium phosphate concentration, $C_{K_3PO_4}$, shown in Fig. 3, illustrates that the average diameter d_N goes through a maximum, which corresponds to the critical aggregation concentration (cac) as the $C_{K_3PO_4}$ varies, although, as it was observed previously [12], it should be constant after the cac of $C_{K_3PO_4}$.

The same anomalous observation, which was also presented previously [20,21], was observed for the variation of the number average diameter d_N of HAP particles with the time at two different concentrations of K_3PO_4 (see Figs. 4 and 5). At the lower electrolyte concentration ($C_{K_3PO_4} = 5\cdot10^{-3}$ M) the maximum average diameter of HAP particles was obtained at about 100 h after the preparation of the sample, while the same time for the potassium phosphate concentration of $1\cdot10^{-2}M$ was lower (~25 h). At the higher $C_{K_3PO_4}$ used ($=5\cdot10^{-2}M$), which corresponds to a concentration higher than the cac, two sample peaks (see Fig. 2) with two different number average particle diameters were obtained and the variation of d_N with the time is shown in Fig. 6. All these observations could be explained by using the Marmur kinetic theoretical approach [22], which is based on the primary and secondary minimum coagulations and their combinations, as follows: the dependence of particle size on the electrolyte concentration or on the time at a constant electrolyte concentration is due to the combination of the two modes (at the primary and secondary minimum) of coagulation. The coagulation for HAP particles in the presence of potassium nitrate (KNO_3) is at the primary minimum [12,22], whereas the coagulation of HAP particles in the presence of potassium phosphate studied in the present work it is at the secondary minimum. Coagulation at the primary minimum for the HAP particles in the presence of

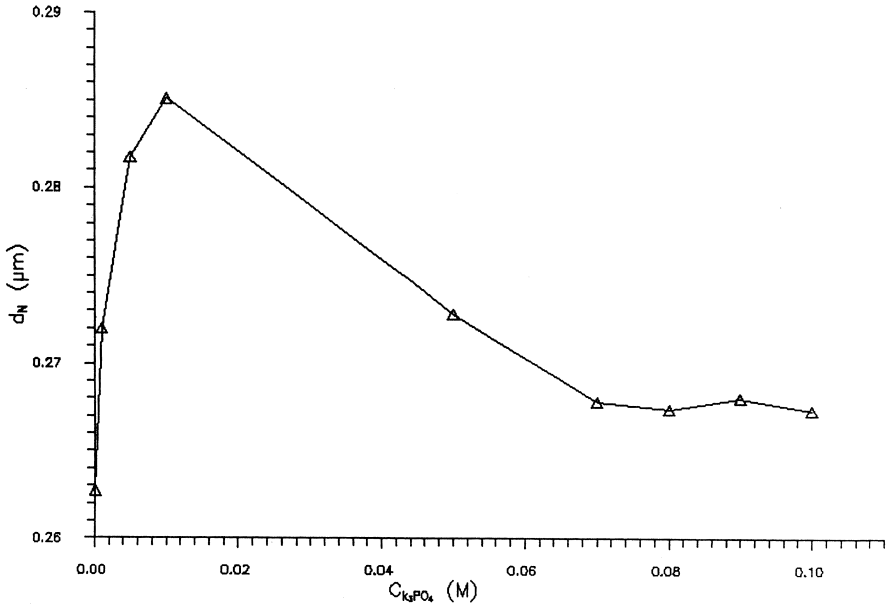

Fig. 3. Variation of number average diameter, d_N, for the HAP particles, obtained by SdFFF with the potassium phosphate concentration $C_{K_3PO_4}$.

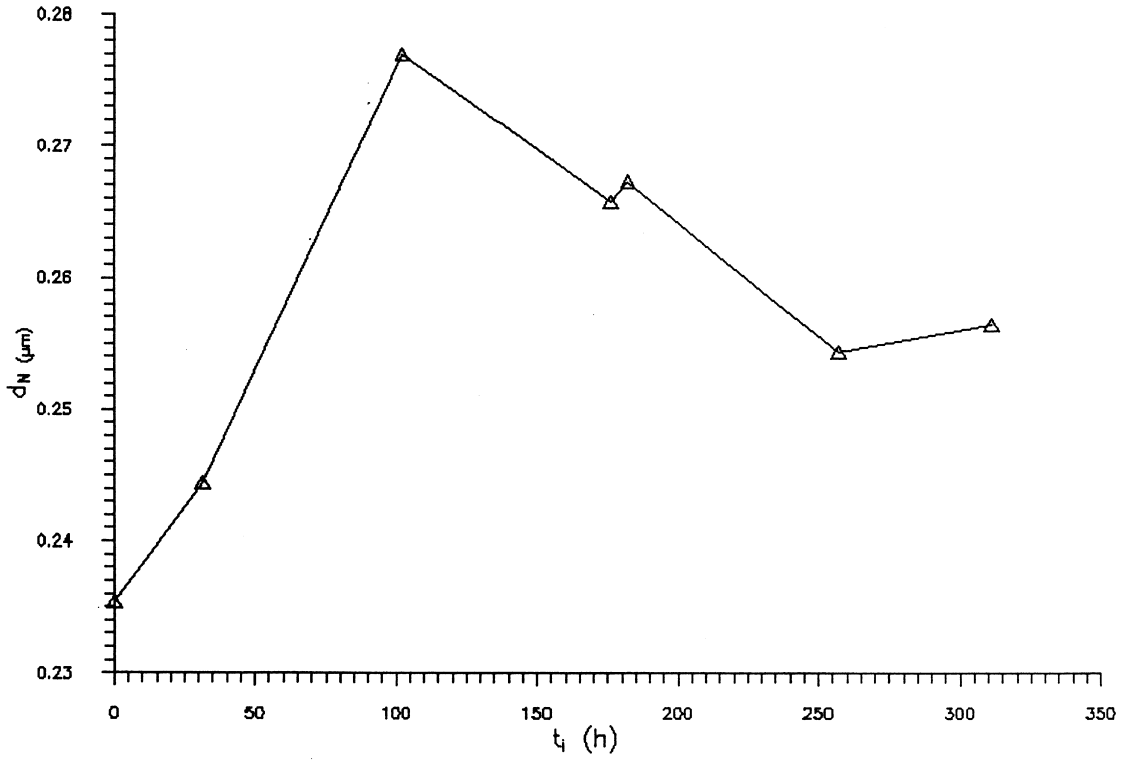

Fig. 4. Time dependence of number average diameter, d_N, for the aggregation process of HAP particles in the presence of $5 \cdot 10^{-3} M$ K_3PO_4.

KNO_3 (see Fig. 3 of [12]) is leading to a steady increase in the diameter d_N as a function of C_{KNO_3} whereas aggregation at the secondary minimum, in the presence of potassium phosphate, produces an increase followed by a decrease in particle size and the heavy flocs formed no longer stay in suspension, possibly due to the reversibility of the second process, though sedimentation (adhesion on the channel surface) of the larger particles could also be a possible cause for the observed decrease in particle size as a function of electrolyte concentration or time. It is interesting to point out that the decrease in d_N is dependent on K_3PO_4 concentration or time and occurs solely above certain levels of added K_3PO_4 or certain times depending on the electrolyte concentration. Because the depth of the secondary minimum increases as a function of electrolyte (K_3PO_4) concentration or time [20], a significant proportion of aggregation at the secondary minimum is only to be expected for the larger particles (corresponding to bigger times) at the highest K_3PO_4 concentrations. These are indeed the conditions to obtain the kinetical profiles for particle size involving a decrease in particle size as a function of electrolyte concentration or time.

All the experimental data of the present work for the aggregation of HAP particles in the presence of K_3PO_4 should be explained, in accordance with the Marmur theory, by the following mechanistic scheme:

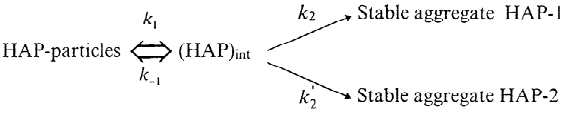

(3)

where $(HAP)_{int}$ is an intermediate complex of HAP, k_1 and k_{-1} are the rate constants for the formation and dissociation of the intermediate complex, and k_2, k_2' are the rate constants for the process of formation of the stable aggregates HAP-1 and HAP-2, respectively. This general mechanistic scheme explains the

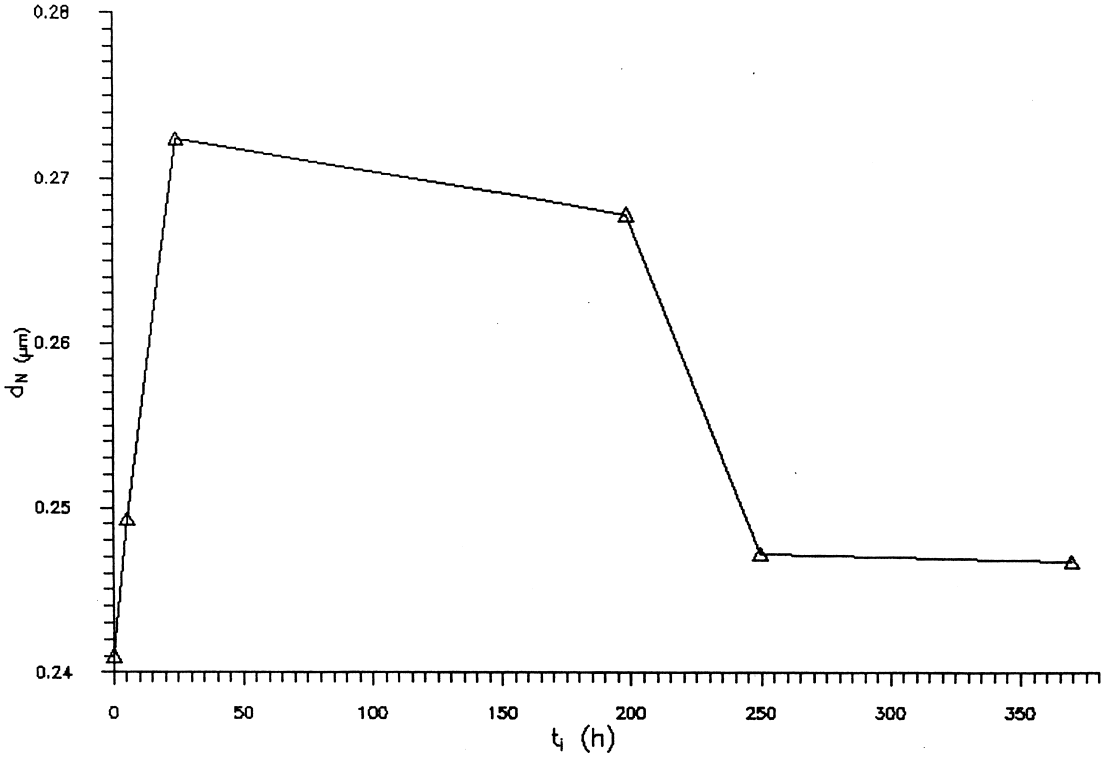

Fig. 5. Variation of number average diameter, d_N, with time for the aggregation process of HAP particles in the presence of $1\cdot10^{-2}M$ K_3PO_4.

two peaks corresponding to the stable aggregates HAP-1 and HAP-2, which appear at times higher than 79 h when the potassium phosphate concentration is $5\cdot10^{-2}$ M (see Fig. 2). The ascending part of the two curves $d_N^{HAP-1}\rightarrow t$ and $d_N^{HAP-1}\rightarrow t$, appeared in the time interval $79<t<100$ h, can be attributed to the aggregation process of HAP particles, which happens when $k_1 \gg k_{-1}$. On the other hand the descending part of the same curves appeared at the time interval $t>100$ h can be attributed to the disaggregation process of HAP particles, which happens when $k_1 \ll k_{-1}$. FT IR spectra (see Fig. 7) verified that both peaks of Fig. 2 correspond to HAP and not to a new substance produced by a reaction from the HAP sample. The above observation shows that the SdFFF technique can divide the polydisperse HAP particles into two narrower fractions, for which subsequent characterization is greatly simplified.

When the two rate constants k_2 and k_2' are not comparable, but $k_2 \gg k_2'$, the general mechanistic scheme presented above is simplified as follows:

$$\text{HAP-particles} \underset{k_{-1}}{\overset{k_1}{\Leftrightarrow}} (\text{HAP})_{\text{int}} \overset{k_2}{\rightarrow} \text{Stable aggregate HAP-1} \quad (4)$$

and one peak is obtained by the SdFFF technique. The ascending part of the curves $d_N \rightarrow C_{K_3PO_4}$ and $d_N \rightarrow t$ ($C=5\cdot10^{-3}$ M, $1\cdot10^{-2}$ M and $5\cdot10^{-2}$ M K_3PO_4 when $0<t<53$ h) can be attributed to the aggregation process of HAP particles, which happens when $k_1 \gg k_{-1}$. On the other hand the descending part of the curves $d_N \rightarrow C_{K_3PO_4}$ and $d_N \rightarrow t$ ($C=5\cdot10^{-3}$ M, $1\cdot10^{-2}$ M and $5\cdot10^{-2}$ M K_3PO_4 when $53<t<79$ h) can be attributed to the disaggregation process of HAP, which happens when $k_1 \ll k_{-1}$.

One of the main disadvantages of normal and steric sedimentation FFF determination of average diameters or particle-size distributions is the foldover

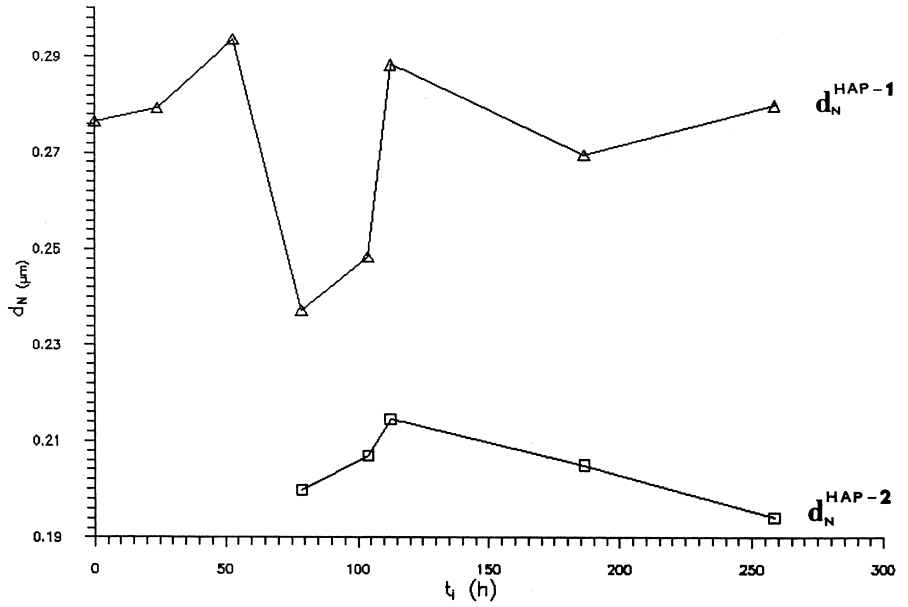

Fig. 6. Variation of number average diameters, d_N^{HAP-1} and d_N^{HAP-2}, with time for the aggregation process of HAP particles in the presence of $5 \cdot 10^{-2} M$ K_3PO_4.

phenomenon when working with a broad-range sample, which spans the foldover point so that particles of different size elute at the same time [23]. Although as a first approximation one could say that the steric effects predominate for particles larger than 1 μm in diameter, the situation of steric effects with particles smaller than 1 μm in diameter is often met for submicron particles when the sedimentation field strength expressed in acceleration, G, and the density difference between particle and carrier, $\Delta\rho$, are very large.

Assuming that the dimensionless steric factor γ, which represents the complication of lift forces and related hydrodynamic effects [23], is constant, the particle diameter at the inversion point from normal to steric FFF is given by the relation [23]:

$$d_i = \left(\frac{36kT}{\pi\gamma\Delta\rho G} \right)^{1/4} \quad (5)$$

while the inversion retention ratio is calculated by the equation [23]:

$$R_i = \frac{4\gamma d_i}{w} = \frac{4}{w}\left(\frac{36\gamma^3 kT}{\pi\Delta\rho G} \right)^{1/4} \quad (6)$$

In our case when $\Delta\rho = 3.155 - 1.000 = 2.155$ g ml^{-1} ($\rho_{HAP} = 3.155$ g ml^{-1}) and $G = 9735$ cm s^{-2}, assuming that $\gamma \approx 1$, Eq. (5) shows that the steric effect predominates with particle diameters larger than 0.688 μm. Taking into consideration that the values of γ range approximately between $0.70 < \gamma < 1.35$ the limiting values of the diameters at the inversion point are $0.639 < d_i < 0.753$ μm. Thus, for the HAP particles the steric effect predominates with particle diameters larger than 0.639 μm. As the TEM pictures show all the longest axes of HAP particles at the experimental conditions used are lower than 0.639 μm, indicating that we are working totally in the normal sedimentation domain, which has been used in the determination of the number average diameters, thus avoiding the foldover phenomenon. The colloidal stability of HAP particles after K_3PO_4 addition, as it was pointed out in Section 2, was characterized by measuring their number average diameters by centrifugal sedimentation FFF as a function of time. The time lag between mixing and the start of the analysis was smaller than a few (~5) min. The apparent rate constant, k_{app}, for the aggregation process of HAP particles, in the presence of potassium phosphate, was calculated as follows:

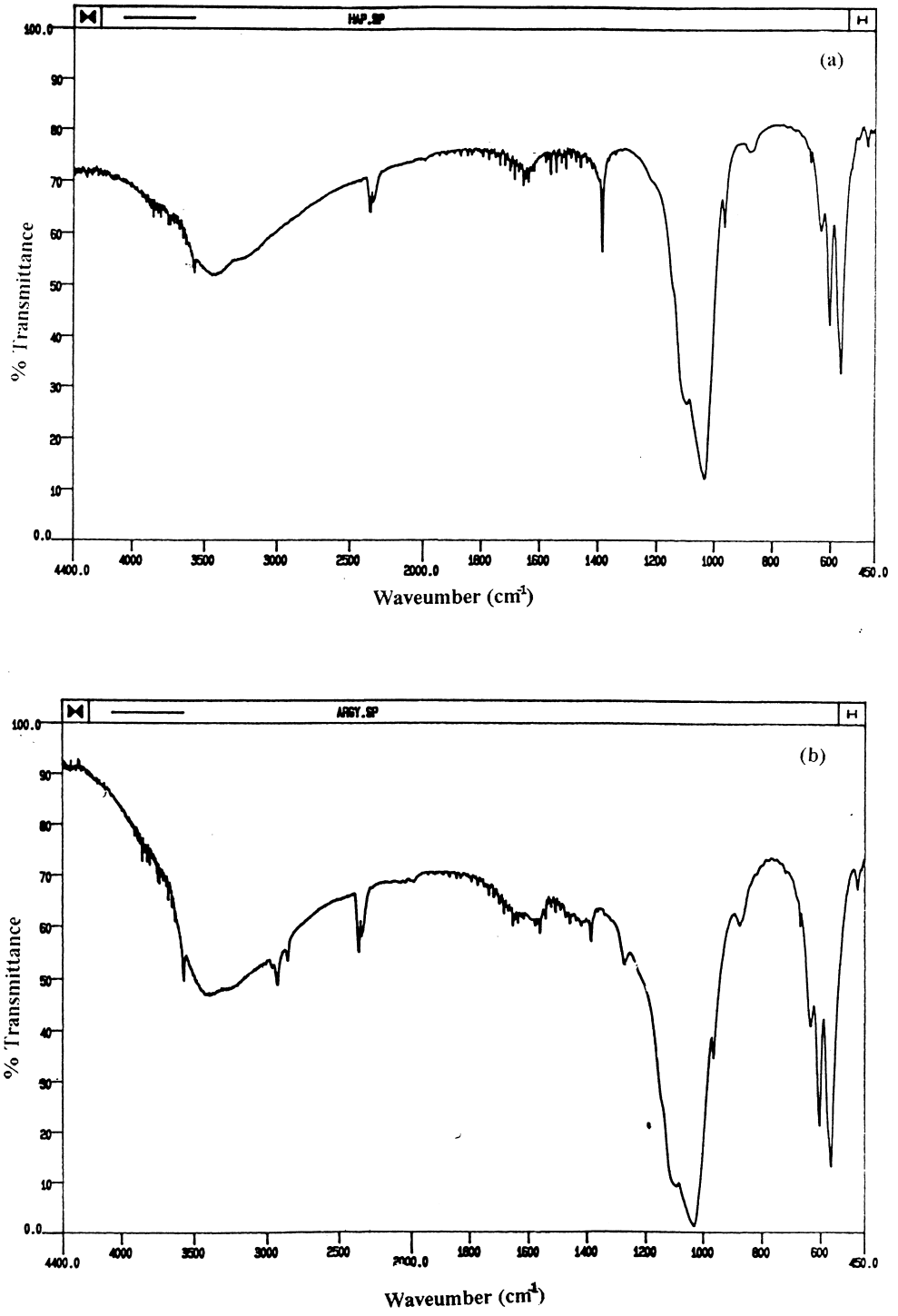

Fig. 7. FT IR spectra of HAP in the presence of $5 \cdot 10^{-2} M$ K_3PO_4: (a) $t = 0$ h; (b) $t = 168$ h.

Both rapid and slow aggregation, in the regions of increased particle size as a function of time, are described by the bimolecular kinetic equation [24]:

$$\frac{1}{N_i} = \frac{1}{N_o} + k_{app} t_i \quad (7)$$

where N_i and N_o are the total numbers of particles per unit volume at times t_i and t_o (initial time), respectively.

Following the procedure described previously for polydisperse samples [12], Eq.(7) yields:

$$d^3_{N_i} = d^3_{N_o} + d^3_{N_o} N_o k_{app} t_i \quad (8)$$

where d_N and d_{N_o} are the measured by SdFFF number average diameters at times $t=0$ and t_i, respectively. A plot of $d^3_{N_i}$ vs. t_i should be linear with an intercept equal to $d^3_{N_o}$ and a slope equal to $d^3_{N_o} N_o k_{app}$, from which the apparent rate constant for aggregation, k_{app}, can be determined. The calculation of the N_o value used in Eq. (8) is described elsewhere [12].

The found values of k_{app} for the aggregation of HAP particles in the presence of three different potassium phosphate concentrations, which are compiled in Table 1, are compared with the k_1 value determined by the Stokes–Einstein relationship:

$$k_1 = \frac{8kT}{3n} \text{ ml s}^{-1} \quad (9)$$

where n is the viscosity of the water, in order to show whether the values of k_{app} are determined by the rate at which two (or more) HAP particles can diffuse up to each other (diffusion control), or whether the rate of reaction is limited by other slower processes. For water at 25°C, using $n=0.97$ cp, we calculate from Eq. (9) a k_1 value of $1.1\cdot10^{-11}$ ml s^{-1}. This value is about nine orders of magnitude greater than the values of k_{app} actually measured. Thus, aggregation rates are slower than those expected if the process was simply diffusion controlled when electrostatic repulsion is absent. Probably, extra repulsive hydration forces [25], occurring at close approach of particles, are involved in the observed slow processes, in accordance with the aggregation mechanistic schemes presented previously. Since k_{app} describing the overall process of aggregation is smaller than the calculated k_1 value, there must be rapid equilibration of the individual particles and their intermediate complexes followed by the slower step of irreversible aggregation, in accordance with the aggregation mechanistic schemes in Eqs. (3) and (4).

As a general conclusion one could say that centrifugal sedimentation FFF can be used with success not only for the kinetic study of the aggregation process of hydroxyapatite particles in the presence of various electrolytes, but also for the division of the polydisperse HAP particles into narrower fractions.

Table 1
Apparent rate constants for slow aggregation (k_{app}) of hydroxyapatite particles in the presence of potassium phosphate determined by SdFFF, and theoretical rate constants for rapid aggregation (k_1) calculated by Eq. (9)

Electrolyte	K_3PO_4		
Concentration (M)	$5\cdot10^{-3}$	$1\cdot10^{-2}$	$5\cdot10^{-2}$
Time interval (h)	$0<t<102.5$	$0<t<24.5$	$0<t<53$
k_{app} (ml s^{-1})	$1.21\cdot10^{-20}$	$3.68\cdot10^{-20}$	$1.18\cdot10^{-20}$
k_1 (ml s^{-1})	$1.1\cdot10^{-11}$	$1.1\cdot10^{-11}$	$1.1\cdot10^{-11}$

Acknowledgements

The authors would like to pay tribute to the services of the late Professor J. Calvin Giddings, who supplied the SdFFF system. They are also grateful to Dr. J.Kapolos, who supplied the hydroxyapatite sample, as well as to Dr. A.Travlos and to M. Barkoula for technical assistance.

References

[1] J.C. Giddings, M.N. Myers, K.D. Caldwell, S.R. Fisher, in: D. Glick (Ed.), Methods of Biochemical Analysis, Vol. 26, Wiley, New York, 1980.
[2] J.C. Giddings, G. Karaiskakis, K.D. Caldwell, M.N. Myers, J. Colloid Interface Sci. 92 (1983) 66.
[3] H.K. Jones, B.N. Barman, J.C. Giddings, J. Chromatogr. 455 (1988) 1.
[4] A. Koliadima, G. Karaiskakis, J. Chromatogr. 517 (1990) 345.
[5] G. Karaiskakis, A. Koliadima, K. Kleparnik, Colloid Polym. Sci. 269 (1991) 583.

[6] A. Koliadima, G. Karaiskakis, Chromatographia 39 (1994) 74.
[7] J. Pazourek, E. Urbankova, J. Chmelik, J. Chromatogr. A 660 (1994) 223.
[8] A. Athanasopoulou, G. Karaiskakis, Chromatographia 43 (1996) 369.
[9] A. Athanasopoulou, A. Koliadima, G. Karaiskakis, Instrum. Sci. Technol. 24 (1996) 79.
[10] A. Athanasopoulou, G. Karaiskakis, J. Liq. Chromatogr. Rel. Technol. 20 (1997) 839.
[11] G. Karaiskakis, A. Athanasopoulou, A. Koliadima, J. Microcolumn Sep. 9 (1997) 275.
[12] A. Athanasopoulou, G. Karaiskakis, A. Travlos, J. Liq. Chromatogr. Rel. Technol. 20 (1997) 2525.
[13] D. Melucci, G. Gianni, G. Torsi, A. Zatoni, P. Reschiglian, J. Liq. Chromatogr. Rel. Technol. 20 (1997) 2615.
[14] K.D. Caldwell, T.T. Nguyen, J.C. Giddings, H.M. Mazzone, J. Virol. Methods 1 (1980) 241.
[15] H. Gilman, D.W.L. Hukins, D.S. Hickey, J. Phys. D.: Appl. Phys. 24 (1991) 127.
[16] A.L. Arsenault, Calcif. Tiss. Int. 43 (1988) 202.
[17] W.H. Boyce, Am. J. Med. 45 (1968) 673.
[18] R.J. Levy, F.J. Schoen, J.T. Levy, A.C. Nelson, S.L. Howard, L.J. Oshry, Am. J. Path. 113 (1983) 143.
[19] D.W.L. Hukins, L.S. Nelson, J.E. Harries, A.J. Cox, C. Holt, J. Inorg. Biochem. 36 (1989) 141.
[20] A.M. Carmona-Ribeiro, J. Phys. Chem. 97 (1993) 11843.
[21] L.R. Tsuruta, M.M. Lessa, A.M. Carmona-Ribeiro, J. Colloid Interface Sci. 175 (1995) 470.
[22] A. Marmur, J. Colloid Interface Sci. 72 (1979) 41.
[23] S. Lee, J.C. Giddings, Anal. Chem. 60 (1988) 2328.
[24] P.C. Hiemenz, Principles of Colloid and Surface Chemistry, Marcel Dekker, New York, 1977.
[25] A.M. Carmona-Ribeiro, L.S. Yoshida, H. Chaimovich, J. Phys. Chem. 89 (1985) 2928.